Enabling Sub-Megawatt Hybrid-Electric Propulsion through High Efficiency Recuperated Inside-out Ceramic Turbogenerator

Benoit Picard, Mathieu Picard, Jean-Sébastien Plante

Exonetik Turbo Inc.
400 rue Marquette
Sherbrooke, Qc
CANADA

benoit.picard@exonetik.com; mathieu.picard@exonetik.com;
js.plante@exonetik.com

David Rancourt

Université de Sherbrooke
3000 boul. Université – Pavillon P2
Sherbrooke, Qc
CANADA

david.rancourt2@usherbrooke.ca

Keywords: hybrid-electric propulsion, eVTOL, high-efficiency engines, ceramic turbines

ABSTRACT

Electric vertical take-off and landing (eVTOL) aircraft propulsion requires new lightweight and efficient power sources to provide tactical advantages over traditional aircraft. Indeed, state-of-the-art simple cycle gas turbine-based generators operate at relatively low Turbine Inlet Temperature (TIT) preventing the reach of sufficient conversion efficiency, particularly when operating at part load. This paper is a feasibility study exploring the potential of a novel ceramic turbine architecture - the Inside-Out Ceramic Turbine (ICT) - that can enable higher TIT while being low-cost and tolerant to monolithic ceramic brittleness by keeping ceramic blades under compressive loads. The analytical aero-thermo model predictions show that, when used as a high-pressure stage of a recuperated cycle, the ICT leads to high on-design fuel-to-DC conversion efficiency of 38%. In addition, unmatched part load efficiency is provided by the synergetic coupling of the recuperated cycle with a variable speed generator, retaining 90% of the rated power efficiency down to 30% load. Although heavier than simple cycle turbogenerators, the gain in efficiency of the ICT-based recuperated system considerably reduces fuel weight at take-off, providing 200% payload improvement on long missions based on a first assessment of this power pack in a 4-passengers eVTOL aircraft. It is also noted that this series hybrid configuration provides 8 times the range of battery-only energy source, which showcases the need for the pursuit of an efficient hybrid power source for the future of military e-aircraft.

1. INTRODUCTION

Recent development of electric propulsion systems for aircraft sparked a renewed interest in multi-rotor and multi-capability vehicle design, proposing advanced capability and tactical advantages for military applications. However, the low energy density of today's and near-term battery technologies allows only very short missions, and requires massive on-ground electrical charging stations whose logistical complexity is often overlooked. Hybrid-electric systems with in-vehicle fuel-to-electric energy conversion could bring the benefits of electric propulsion without compromises on vehicle range. Developing aircraft hybrid-electric generators presents a substantial engineering challenge as generators must be both power dense and highly efficient at the same time, a characteristic hardly met by any fuel-conversion system seen today. For aircraft with power needs below 400 kW, internal combustion (IC) engines lead the market due to their high efficiency and reduced cost. However, efficient piston-based engines remain heavy, cannot operate on kerosene, and have low reliability compared to gas turbines.

Between 400 kW and about 4 MW, turboshafts and turboprops based on simple Brayton cycle are commonly used in military applications. Although lightweight, these engines have low thermal efficiency due to their low-pressure ratio and limited turbine temperature capability. Simple cycle turbines are also known for their high fuel consumption in part loads, therefore less suited for eVTOL applications where peak-to-cruise power ratio would be higher than classical helicopters.

Sub-megawatt turbomachine energy conversion efficiency could be drastically improved by recovering the exhaust gas energy with a heat exchanger (HX). Interestingly for VTOL applications, the efficiency gain of the recuperated Brayton cycle becomes even larger in part load operations (Kim and Hwang, 2006). Recuperated turbines also bring noise attenuation and reduced heat signatures, other important advantages for military applications. Up to now, the introduction of recuperated turbines in aircraft has been hindered by its large mass and thermal stresses imposed by transient requirements that can lead to heat exchanger distortion and cracking (McDonald et al., 2008). While the imposed transient requirements remain a potential challenge for the certification of a recuperated engine for conventional propulsion systems, the hybridization provides a synergetic solution to this problem since the transients of a turbogenerator can be adjusted by coupling the system with an electrical energy buffer. The load requirements can therefore be controlled similarly to the ones of ground power system where HX operates for over 30 000 hours without failure.

The remaining challenge for recuperated cycle in an airborne turbogenerator application is the current mass of commercial recuperators used for ground power generation. Improving the specific power output of the turbine is the key to increasing power output while limiting the size of the HX. To improve the specific power, the Turbine Inlet Temperature (TIT) must be increased above the one of commercial sub-megawatt turbines that typically incorporate uncooled metallic blades. At this scale, introducing blade cooling is costly and defeats the purpose of a recuperated cycle as the cooling flow is inevitably mixed with the main flow and reduces the exhaust temperature available for recuperation. As an alternative, using better turbine materials for small recuperated gas turbines is seen as the most promising strategy. Ceramics is often suggested as the leading material candidate. However, extensive work on conventional rotors designed with monolithic ceramics proved to be unreliable due to crack propagation leading to catastrophic rotor failure (Sakakida et al., 1994; Takehara, Tatsumi and Ichikawa, 2002; Roode, Ferber and Richerson, 2002). To improve the fracture toughness of ceramics, the industry is heavily investing in ceramic matrix composites (CMCs). CMCs have successfully been introduced in static parts of the CFM LEAP engine in 2016, and are expected to be largely used in the GE9X hot section in 2020 (Zok, 2016), however, only for static components. Current CMCs do not have the required strength for long life rotating components of large-scale gas turbines (van Roode, 2009), and the adaptation of the CMCs technologies to be functional and cost effective in small gas turbine rotating parts is therefore not foreseen in the near future.

Exonetik's Inside-out Ceramic Turbine (ICT) configuration, shown in Figure 1-1, provides an alternate approach that allows the use of low-cost monolithic ceramics into small gas turbines by supporting the blades with an outer rotating composite rim made of carbon fiber and polyimide matrix. An air-cooled insulation layer is placed between the blades and the composite rim to prevent the blade's heat to reach the composite. This architecture keeps the independent blades under compression by centrifugal forces. The feasibility of the ICT has been demonstrated with proof-of-concept prototypes in previous papers from the authors (Landry et al., 2016; Courtois et al., 2017). System modeling of a CHP application with the ICT showed a thermal efficiency capability of 45% at a power of 240 kW (Kochrad et al., 2017). To further evaluate the potential of a recuperated ICT for aircraft applications, a trade-off study between power density and efficiency was conducted to select the optimum HX sizing and pressure ratio at different TIT levels (Picard et al., 2019). In this sizing for a turboprop application, the selected optimal ICT turbine along the Pareto front generated for 1550 K TIT reached a thermal efficiency of 40%

at a power density of 3 kW/kg. This selected engine requires a pressure ratio of only 8.3, achievable with a single stage radial compressor and two-stage axial turbines.

One of the possible turbogenerator architecture based on such configuration is shown in Figure 1-1, with single spool arrangement leading to low system complexity. For compactness and reliability, the generator is directly driven by the turbines (i.e. no gearbox), entering the speed regime of the ultra-high-speed generator (UHSG). For the proposed short-term target with a TIT of 1550 K, the ICT serves as the high-pressure turbine, and the low-pressure turbine is metallic, followed by a metallic recuperator. Previous studies have focused on predicting ICT engine performance for on-design operations, without considering the application at the system-level (Kochrad et al., 2017). There is therefore an interest in better understanding the benefit of a high-temperature recuperated turbine in a relevant hybrid-electric aircraft application, including the effect of off-design operations. To address this question, this paper presents a feasibility study aiming to explore the expected performance of a recuperated turbogenerator implementing high Turbine Inlet Temperature (TIT) with a newly developed ceramic turbine – the Inside-out Ceramic Turbine (ICT) – directly coupled with an ultra-high-speed generator (UHSG). Off-design performance of different architecture candidates for series hybrid vehicles are first compared. The best architecture is then selected for both recuperated and simple cycles and their potential on a 4 passengers eVTOL is compared in terms of payload and range.

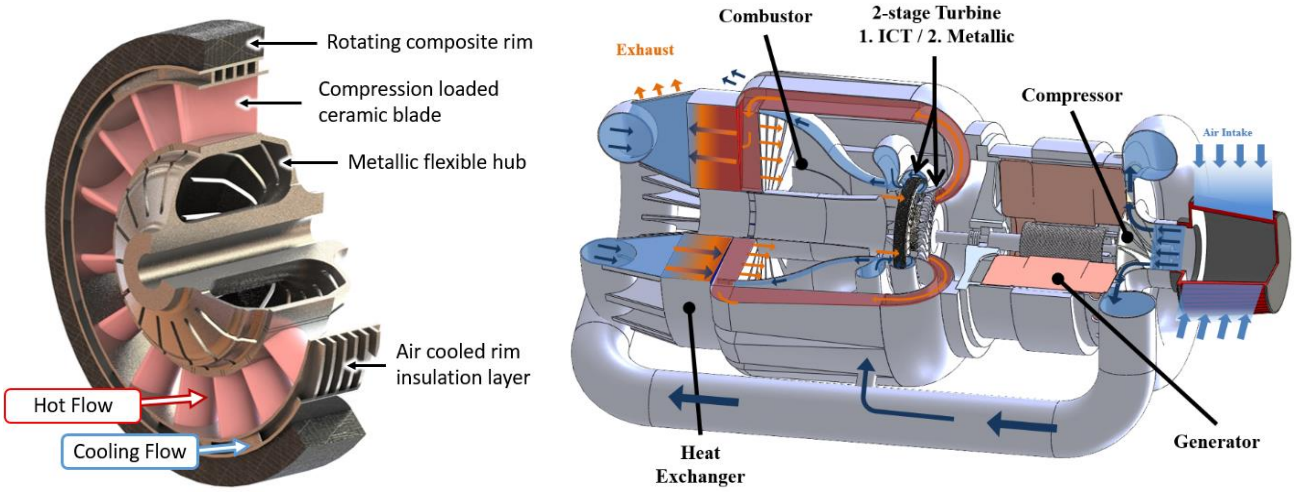

Figure 1-1 – Exonetik demonstrated Inside-out Ceramic Turbine prototype (left) and turbogenerator conceptual architecture (right)

2. TURBOGENERATOR CONVERSION EFFICIENCY VS POWER DENSITY

The optimum engine design for an aircraft payload and range fundamentally faces a trade-off between the conversion efficiency and its power density. As the efficiency is increased, less fuel is required for take-off and the weight of the engine can be increased while maintaining the vehicle payload capacity. This section will therefore evaluate this trade-off on both recuperated and simple cycle sub-megawatt turbines considering their nominal performance at ground level (on-design). In this study, a set of design variables are selected to primarily quantify the impact of higher TITs, pressure ratios and recuperator sizing on the engine performance. Although

performance metrics to entirely define the added value of a given power system is far more exhaustive, quantitative evaluation will be limited to efficiency and power density for the present study.

The on-design efficiency and power density are typically the most important metric linking the engine to the aircraft payload and range capabilities. However, in application where idle or part load operation represent a significant amount of the total operation time, off-design relative efficiency becomes an important metric affecting the final aircraft capabilities. As the off-design relative efficiencies are different for the two types of cycle, further investigation into the part load performance is also completed for four possible engine architectures. The relative efficiency curve obtained is then used in the following section to establish aircraft performance. The transient behavior of the system and its impact on the payload and range capabilities are assumed negligible, therefore only steady-state off-design conditions are analyzed.

2.1. On-Design Performance

In order to obtain the trade-off between power density and efficiency of the turbogenerator, modeling of the conversion efficiency and weight of each subsystem based on selected design variable is first completed. The fuel-to-shaft power conversion is based on standard station-based thermodynamic model incorporating specific losses such as drag, cooling and sealing for the ICT configuration, and a one-dimensional finite element model (1D-FEM) computes heat and mass transfer for straight counterflow recuperator channels providing its pressure losses, thermal effectiveness and specific mass. An empirical relation built between existing turboprop and turboshaft weight and their rated power at their associated inlet air mass flow obtains the mass of the turbine. The HX weight is then added to obtain the total turboshaft weight. Both submodels, detailed subfunctions and validation are available in a recent publication by the authors (Picard et al., 2019), together with system optimization for the thermal efficiency vs power density of a turboprop configuration.

To establish turbogenerator fuel-to-electricity efficiency and power density, the electrical generator and power electronics specifications are taken to adjust the previous turboprop optimization results. Direct Drive Ultra-High-Speed Generator (UHSG) brings high generator power density potential while also removing the needs for the traditional turboprop gearbox. However, extracting copper and iron losses in their compact geometries makes high efficiency harder to achieve than in low-speed motors. Limited literature is available on UHSG efficiency vs. power density trade-offs, but based on the author's research, an electrical efficiency of 97% is assumed achievable in the near future at power density reaching 15 kW/kg. To minimize power electronics losses at the very high switching frequency required, SiC MOSFETS used in an active rectifier combined with improve filtering and packaging components are expected to provide AC-to-DC conversion efficiency of 98% at a power density of 16.4 kW/kg (Dever et al., 2015). Those electrical conversion efficiencies multiply the thermal efficiency to obtain total fuel-to-DC conversion efficiency.

The resulting trade-off for 3 TIT levels and the two engine types are presented in Figure 2.1-1. Each of the dots on those Pareto fronts actually represent different engine design, changing TIT, pressure ratio and HX geometries. A TIT of 1300 K represents state-of-the-art uncooled metallic turbines; 1550 K is the short-term objective for ICT turbine achievable with commercially available ceramic materials and metallic recuperator; and 1800 K is the long-term development objective with advance materials. The turbogenerator with the ICT proposed in Figure 1-1 would reach a system power density of 2.5 kW/kg at a conversion efficiency from fuel-to-DC of 38%.

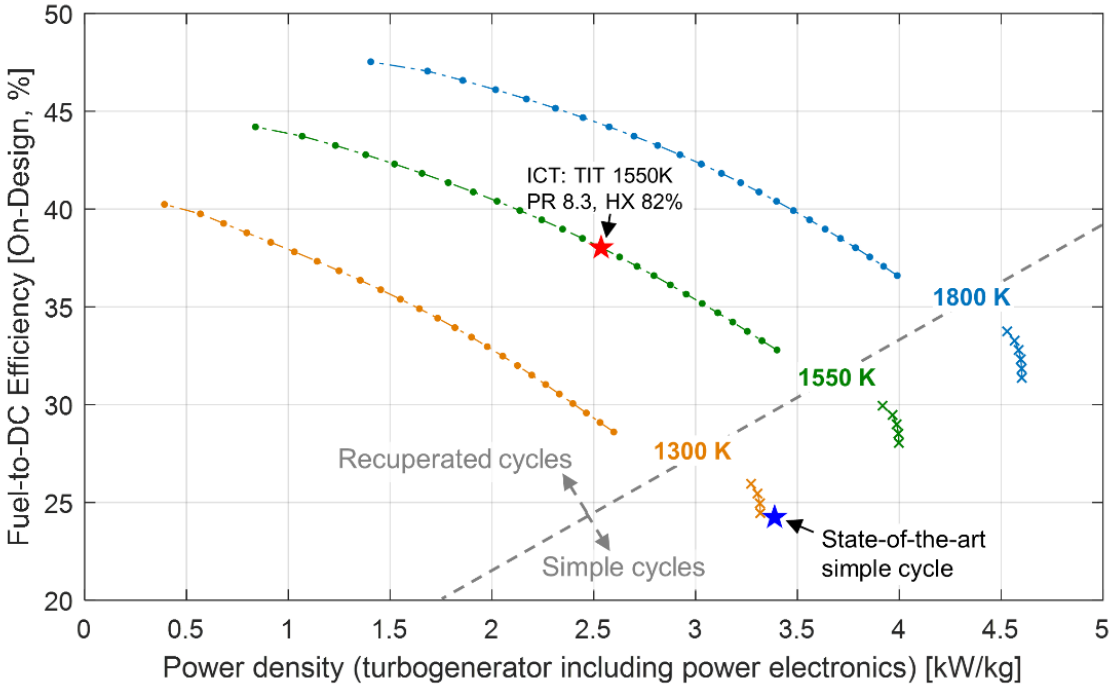

Figure 2.1-1 – Pareto fronts showing achievable conversion energy versus power density of the turbogenerator power pack for both recuperated and simple cycle systems at TIT levels. Engine design varied: compressor pressure ratio and recuperator design geometries

2.2. Off-Design Performance

Sub-megawatt turboprops and turboshafts from nearly all engines manufactures have converged on two-spool free-turbine architecture. This arrangement allows larger torque capacity versus a single spool and is easier to start by being decoupled from the load – a must for helicopter large rotors. However, replacing conventional gearbox with high-speed generator that can control the braking speed and load while also acting as a starter motor change the design requirements and the optimum architecture for series hybrid systems is therefore challenged. The four configurations shown in Figure 2.2-1 are therefore suggested as candidates; single or two spools, both with or without recuperation. Two operation methods are also evaluated in order to compare the variable speed capability introduced by the generator to conventional fixed speed rotor operations. Although the model can predict high altitude performance, only sea-level part load performance will be presented here since the eVTOL application later discussed is expected to operate at low altitude.

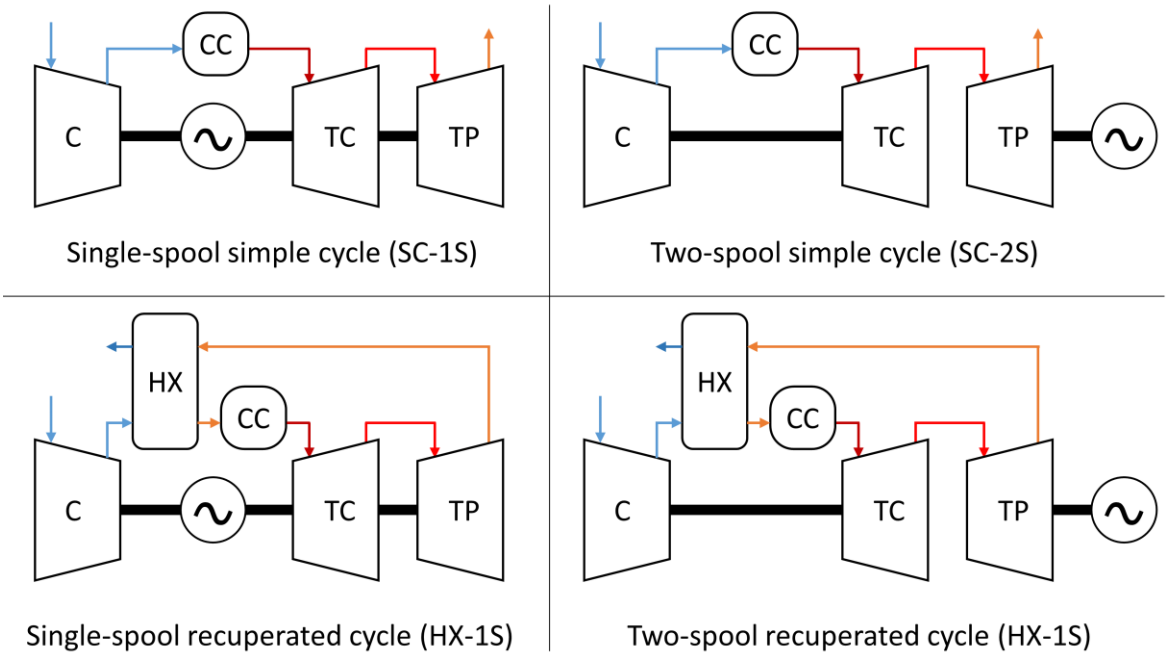

Figure 2.2-1 – The four (4) architectures studied for optimal series hybrid engines [C: Compressor, TC: Compressor Turbine (high pressure), TP: Power Turbine (low pressure), HX: Heat Exchanger, CC: Combustion Chamber]

2.2.1. Methodology

Part load performance analysis is based on experimental compressor and turbine components maps (Saravanamuttoo et al., 2008; Haglind and Elmegaard, 2009). Although engine OEM do not publish their maps, studies in the open literature have presented numerous maps, and were compiled in GasTurb 13 commercial software (Kurzke, 2013). To avoid numerical resolution challenges for vertical regions of the maps (constant corrected flow when choked), introduction of auxiliary coordinates β are used (Kurzke, 1996). Careful selection of the best corresponding map in terms of pressure ratio and mass flow was made – within the limited available maps for small gas turbines – and then scaling by traditional methods (Sellers and Daniele, 1975) is applied based on the on-design point. Additional modeling information is available in a recent publication by the author (Picard, 2019).

Part load operation has a positive effect on the HX performance by reducing the volumetric flow and therefore reducing the pressure losses. Its thermal effectiveness is also increased due to the increased residence time. The HX 1D-FEM model developed for on-design calculation is also used to account for those effects when solving off-design points. To obtain the combustion efficiency of the combustor at part load, model based on burner loading relation (Münzberg and Kurzke, 1977), and classical log-log slope coefficient of 1.6 is used based on the JT8D turbine reference data. Mechanical efficiency and thermal losses are applied with the same percentage as the on-design model. Both the generator and power electronics are expected to improve their efficiency at reduced load and speeds. To stay conservative, and since the variation would be not impact the overall system significantly, no correction to the efficiency in off-design is applied to these components.

The resolution of each off-design point is solved at a sweep of reduced fuel flow with a constrained multi-variable non-linear optimizer (*Matlab fmincon*). The inlet mass flow, the HX air-side heat ratio, the relative speed of each spool and β coordinates for each component map are varied in order to obtain a valid point in which inlet and exit pressure matches, corrected mass flow for each component match their respective maps and the cycle HX effectiveness match the HX 1D submodel prediction. Additional constraints are added to first respect a surge margin of at least 10%, second to limit TIT and HX inlet temperature to the design values and lastly, for two spools free turbine arrangement, to match compressor power and high-pressure turbine power. Finally, the optimization objective is either set to minimize speed deviation from the on-design speed (fixed speed operation), or set to maximize conversion efficiency (variable speed operation).

2.2.2. Off-Design Model Validation

Existing turbine performance numbers are used to validate the off-design model. The single spool recuperated turbine Capstone C250 data from the manufacturer (Meybodi and Behnia, 2012) and the two-spool simple cycle PT6A-67P data extracted from the PC-12 NG pilot handbook at ground level (PILATUS AIRCRAFT LTD., 2010) are used as reference. References for literature component maps used are given in Table 2.2.2-1, and comparison between manufacturer data and model predictions is shown on Figure 2.2.2-1. Errors below 1.5 points of efficiency are found from 30% load and above. Errors are relatively larger at lower loads, and are mainly attributed to larger compressor map misrepresentation in that area. Idle estimates are optimistic for both types of engines with this method, nevertheless, the difference between recuperated and simple cycle is well captured.

Table 2.2.2-1 – Components map used for validation of C250 and PT6A engines

Engine	Component	Reference	On-design point			
			β	N_{rel}	η_{is}	PR
C250	Radial compressor	NASA, 1977 (Klassen, Wood and Schumann, 1977)	0.7	0.95	82.5	5.0
	Radial turbine	NASA, 1984 (Coverse, 1984)	0.7	1	87.4	4.5
PT6A	Axial-radial compressors	RR Allison 250	0.6	0.95	80	10
	Axial turbines (2 stages) (same map for both)	US Army, 1968 (Schober and Franklin, 1968)	0.7 0.6	1 1	86 86	3.3 2.8

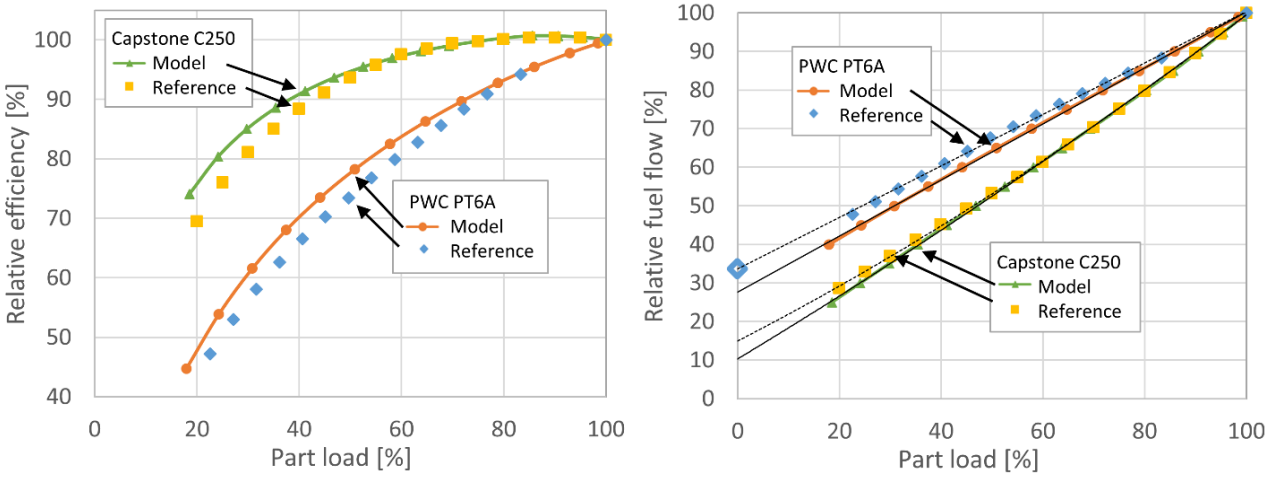

Figure 2.2.2-1 – Model validation on recuperated and simple cycle engine; relative efficiency [left], relative fuel flow [right] (both relative to on-design, i.e. 100% load values)

2.2.3. Off-Design Performance

To compare the different architectures and control methods, two configurations at a TIT of 1550 K are chosen from the on-design results Pareto front. Component map reference for this comparison as well as the design point selection and performance are shown in Table 2.2.3-1. The higher pressure ratio required for the optimal simple cycle requires a multistage compressor, opposed to the single radial compressor for the recuperated cycle.

Table 2.2.3-1 – Nominal performance and components map used for the comparison of the recuperated and the simple cycle engine on the proposed architectures

Engine	Component	Reference	On-design point				Performance	
			β	N_{rel}	η_{is}	PR	η_{elec}	PWD
HX 1S or 2S VS or FS	Radial compressor	NASA, 1977 (Klassen, Wood and Schumann, 1977)	0.6	1	80	8.3	38%	2.5 kW/kg
	Axial turbines	US Army, 1968 (Schober and Franklin, 1968)	0.7 0.6	1 1	90 88	2.4 3.0		
SC 1S or 2S VS or FS	Axial-radial compressor	RR Allison 250	0.6	0.95	80	13.0	29%	4.0 kW/kg
	Axial turbines	US Army, 1968 (Schober and Franklin, 1968)	0.7 0.6	1 1	90 88	3.1 3.8		

The off-design conversion efficiency and the relative efficiency of the on-design point for the 4 configurations and 2 operation methods are compared in Figure 2.2.3-1. To explain the major differences between the configurations, the associated operational values for TIT and compressor efficiencies are shown in Figure 2.2.3-2. The legend refers to the number of spools (1S or 2S) and the operation method (fixed speed FS, variable speed VS) for both recuperated cycle (HX) and simple cycle (SC). The architecture with a recuperator on a single spool and variable

speed control (1S-VS) clearly provides the best part load conversion efficiency. It can maintain upward of 90% of its on-design efficiency down to nearly 30% load. This gain can be mainly attributed to the capability to maintain high TIT in part load without wasting exhaust heat, with another benefit coming from the control of optimal compressor efficiency. Efficiency deteriorates more rapidly for a single spool fixed speed (1S-FS) on both cycle type, and especially drastically for the recuperated cycle. Finally, in the case where concerns arise from the recuperated single spool arrangement not reaching the maximum achievable turbine stages efficiency due to blade speed constraints, a dual spool with generators on each of them would provide the same cycle performance and potentially better control, although increasing system complexity.

The system architecture with leading part load efficiency is then selected for each cycle type and a second order regression based on the relative fuel flow and relative power is made. Those regressions are then used for the vehicle-level calculations, saving computational time while introducing very limited error. Aircraft speed and altitude effects on fuel flow are assumed negligible considering the limited altitude and vehicle speed of the eVTOL platform studied.

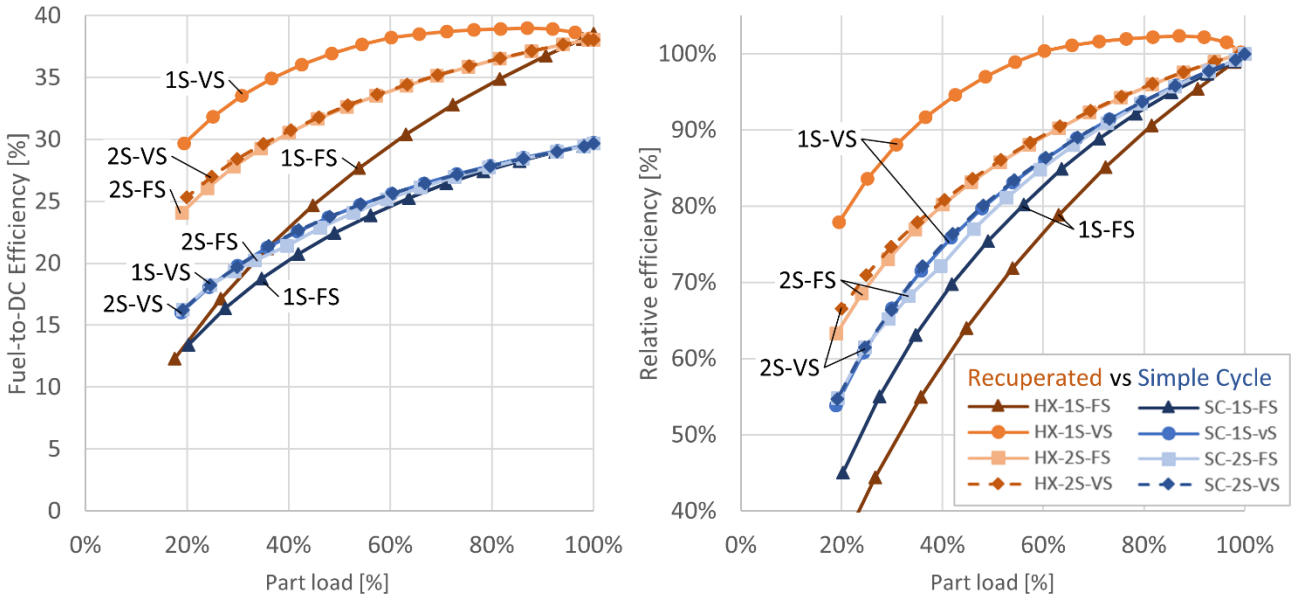

Figure 2.2.3-1 – Efficiency comparison for the 4 architecture with fixed and variable speed operations; conversion efficiency [left], efficiency relative to on-design [right]

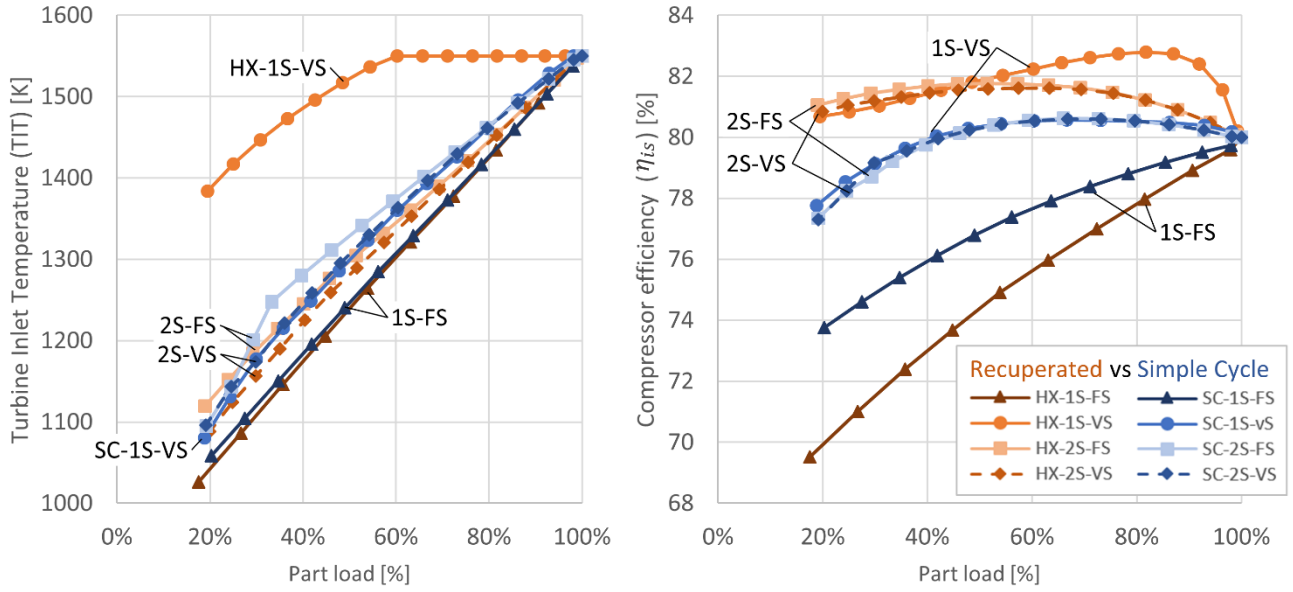

Figure 2.2.3-2 – Turbine inlet temperatures [left] and compressor isentropic efficiency [right] against load ratio for the 4 architectures with fixed and variable speed operations

3. EVTOL CAPABILITIES EXPLORATION WITH TURBOGENERATOR

The new capabilities provided by electric powertrain aircraft have sparked a renewed interest in advance vehicle configuration. The lingering goal is to have a vehicle with VTOL capability while cruising at fixed-wing speeds. For the purpose of this paper, the tilt-rotor eVTOL vehicle (*Figure 3-1*) detailed in a sizing studied published by The Boeing Company (Duffy, Wakayama and Hupp, 2017) is selected in order to establish the optimum turbine technology for this type of aircraft. This eVTOL was designed around an air taxi application that travels 160 km (100 miles) with 363 kg (800 lbs) nominal payload capacity (4 passengers) for a gross take-off weight of 1782 kg. The mission power profile is shown on *Figure 3-1*, requiring a hovering power of 407 kW (sea level, ISA+0) and a cruise power of 140 kW, values considered as DC power exiting the power source.

Although not specifically designed for military missions, it is presumed that such a vehicle would achieve significant tactical advantage if sufficient range and payload capabilities were to be met. The reference analysis by Boeing is based on battery-only energy source, having 154 kWh of energy onboard by stocking 440 kg of 400 Wh/kg li-ion batteries, which is the expected energy density of li-ion cells in 2030 by NASA (Dever et al., 2015), with an expected 15% pack burden. From the mission power profile, the vehicle requires 132 kWh of energy per mission while having a 22 kWh reserve capacity.

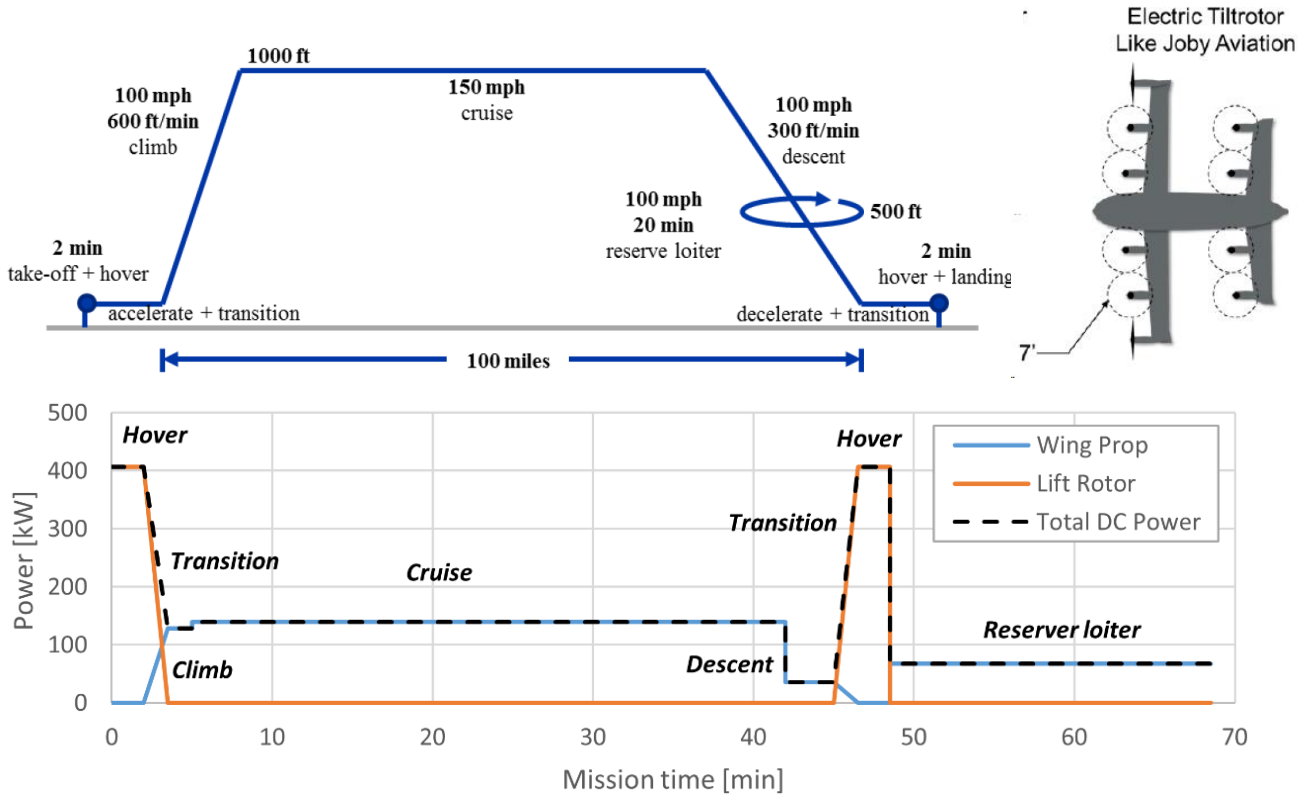

Figure 3-1 – Tiltrotor eVTOL mission profile over the 160 km mission [left], vehicle aerial sketch [right] and electric power profile [bottom] (adapted from (Duffy, Wakayama and Hupp, 2017))

3.1. Hybrid-Electric Mission Capacity Methodology

The proposed alternative is to keep the entire vehicle and electric propulsion system, but replace the 440 kg of batteries by a fuel-based turbogenerator power source. As a first exploration step, the turbogenerator is sized to supply the entire hovering power. This provides robustness by ensuring sustained hovering capability and would allow the vehicle to cruise at higher power if higher speeds are needed. Also, note that the following requirements are neglected at this stage of the exploration: take-off over nominal power (high temperature and high altitude), transient and emergency energy storage, and component redundancy.

To establish the potential of the engines along the Pareto front presented in Figure 2.1-1, two aspects of the vehicle performance are evaluated with each of those engines; the number of mission blocks that can be achieved at a fixed payload, and the payload achievable for a fixed number of consecutive missions. Iteratively for each engine, the mission fuel burn is first obtained as follows:

1. Obtain the rated power fuel flow from the nominal power and on-design efficiency (assuming the use of kerosene with a lower heating value (LHV) of 43 MJ/kg)

2. Split the mission cycle into a second-by-second power curve and obtain the power ratio for each point

3. Apply the off-design relative fuel flow regression from section 2.2.3 at each second-by-second point

4. Multiply by the nominal fuel flow and integrate over the mission block (same process is completed for the reserve fuel)

To obtain the fuel capacity, the turbogenerator and power electronics mass, the reserve fuel and the fuel tank mass (approximated to 10% of the fuel capacity) are removed from the 440 kg of allowable energy source mass. Dividing this fuel capacity by the single mission fuel burn, the achievable mission count on a single refueling is obtained. The payload capacity is also of interest as a trade-off with the fuel weight. Therefore, based on the same mission fuel burn, the payload capacity with sufficient fuel to run 8 times the mission consecutively is calculated.

3.2. Payload and Mission Capability

The vehicle range and payload capability for a variety of engine performance are made by superposing the engine Pareto trade-off and the mission results contour lines. Figure 3.2-1 presents both the mission count capacity for a payload fixed at the nominal capacity of 363 kg, and the payload capacity fixing the mission count at 8 (for a total of 1280 km including 8 vertical take-off & landing). The expected capacity for a state-of-the-art simple cycle turbogenerator would be 4.4 mission count for the nominal payload, or could achieve 8 consecutive missions by reducing the payload to a third of its nominal value (120 kg, or -67%). The proposed recuperated ICT turbogenerator with a TIT of 1550 K would reach a mission count capacity of 8 at the nominal payload, therefore increasing the vehicle range by 80% compared to state-of-the-art simple-cycle engines for this payload. It can be appreciated how recuperated cycles for a given TIT provides a significant improvement for this eVTOL mission load profile, which is related to their part load improvement. To iterate once more, optimistic battery-electric arrangement with a technology horizon of 15 years is expected to fulfill a single mission at the nominal payload.

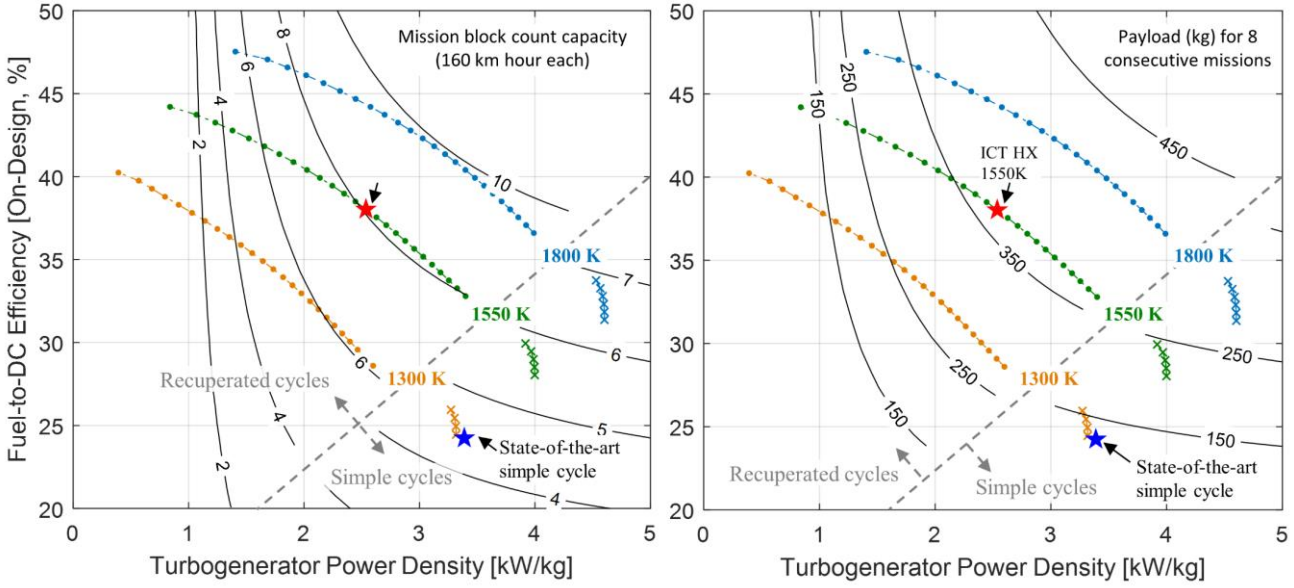

Figure 3.2-1 – Mission block count capacity (160 km each) at a fixed 363 kg of payload [left] and the payload at a fixed mission count of 8 [right] for a 4-passenger tilt-rotor eVTOL

4. CONCLUSION

Today's electrical energy storage technologies have poor energy density, providing battery-only aircraft systems poor range and payload capability against current liquid fueled aircraft. Converting fuel to electricity directly on board would provide significant improvement in energy storage capacity while providing new engines and aircraft architecture advantages. The proposed new turbine architecture, referred as Inside-out Ceramic Turbine, provides a reliable architecture that uses low-cost monolithic ceramic blades by loading them in compression and alleviating impact damage and fragile cracking failure mode. Combining the modeled recuperated engine performance at a TIT level of 1550 K with high power density electric motor and power electronics, a DC power source with 38% conversion efficiency and 2.55 kW/kg power density is predicted. In addition to the gain in on-design efficiency over simple cycle, the recuperated cycle operating in a single-spool engine with variable speed control provides a significant improvement in part-load relative efficiency compared to simple cycle turbines by avoiding high exhaust energy losses. The proposed optimal configuration maintains upward of 90% of its on-design efficiency down to 30% load. Those results show the synergetic combination of the integration of a recuperator, a speed-controlled generator and the high temperature ceramic turbine to achieve a high-performance power source.

The battery pack of a conceptual all-electric aircraft was replaced with a hybrid turbine-based power source in order to showcase the performance of such systems on payload and range. A 4-passenger tilt-rotor aircraft based on Boeing conceptual study was selected in order to demonstrate the challenges of simple cycle with high power ratios between hovering and cruise (peak power around 3 times the cruise power). It was found that the ICT in a recuperated cycle at a TIT of 1550 K provides a capability of 8 consecutive 160 km (100 miles) mission at the nominal payload of 363 kg (800 lbs) before refueling, which is an increase of 80% above the range capability of a state-of-the-art simple cycle gas turbine-based generator at such payload. Alternatively, when comparing at a fixed range given by 8 consecutive missions achieved by trading payload for fuel, the ICT in a recuperated cycle provides a 200% increase in payload capability over the state-of-the-art simple cycle propulsion system.

Finally, while the ICT engine development progresses in order to reach the modeled performance, exploration of eVTOL design best suited to the high on-design and part-load efficiency would allow to find the best synergetic aircraft and power source arrangements for specific applications.

5. REFERENCES

Courtois, N. et al. (2017). Superalloy Cooling System for the Composite Rim of an Inside-Out Ceramic Turbine. In: *Proc. of the ASME Turbo Expo 2017: Turbomachinery Technical Conference and Exposition*. Volume 8: Microturbines, Turbochargers and Small Turbomachines; Steam Turbines. 26 June 2017. Charlotte, NC USA: ASME. p.10. [Online]. Available at: doi:xxx.

Coverse, G. L. (1984). *Extended parametric representation of compressor fans and turbines. Volume 2: Part user's manual (parametric turbine)*.

Dever, T. P. et al. (2015). *Assessment of Technologies for Noncryogenic Hybrid Electric Propulsion*.

Duffy, M. J., Wakayama, S. R. and Hupp, R. (2017). A study in reducing the cost of vertical flight with electric propulsion. In: *17th AIAA Aviation Technology, Integration, and Operations Conference*. 2017. p.3442.

Haglind, F. and Elmegaard, B. (2009). Methodologies for predicting the part-load performance of aero-derivative gas turbines. *Energy*, 34 (10), pp.1484–1492.

Kim, T. S. and Hwang, S. H. (2006). Part load performance analysis of recuperated gas turbines considering engine configuration and operation strategy. *Energy*, 31 (2), pp.260–277. [Online]. Available at: doi:10.1016/j.energy.2005.01.014.

Klassen, H. A., Wood, J. R. and Schumann, L. F. (1977). *Experimental performance of a 16.10-centimeter-tip-diameter sweptback centrifugal compressor designed for a 6: 1 pressure ratio*.

Kochrad, N. et al. (2017). System-Level Performance of Microturbines With an Inside-Out Ceramic Turbine. *Journal of Engineering for Gas Turbines and Power*, 139 (6), pp.062702-062702–062710. [Online]. Available at: doi:10.1115/1.4035648.

Kurzke, J. (1996). How to get component maps for aircraft gas turbine performance calculations. *ASME paper*, (96-GT), p.164.

Kurzke, J. (2013). *Compressor and turbine maps for gas turbine performance computer programs*. [Online]. Available at: http://www.gasturb.de/.

Landry, C. et al. (2016). Development of an Inside-Out Ceramic Turbine. In: *Proc. of the ASME Turbo Expo 2016: Turbomachinery Technical Conference and Exposition*. 8. 13 June 2016. Seoul, South Korea: ASME. p.V008T23A022. [Online]. Available at: doi:10.1115/GT2016-57041.

McDonald, C. F. et al. (2008). Recuperated gas turbine aeroengines. Part III: engine concepts for reduced emissions, lower fuel consumption, and noise abatement. *Aircraft Engineering and Aerospace Technology*, 80 (4), pp.408–426.

Meybodi, M. A. and Behnia, M. (2012). A study on the optimum arrangement of prime movers in small scale microturbine-based CHP systems. *Applied Thermal Engineering*, 48 (Supplement C), pp.122–135. [Online]. Available at: doi:10.1016/j.applthermaleng.2012.05.013.

Münzberg, H.-G. and Kurzke, J. T. (1977). *Gasturbinen: Betriebsverhalten und Optimierung*. Springer.

Picard, B. (2019). Optimisation de turbines à gaz en céramique récupérées pour des applications aéronautiques. *Université de Sherbrooke*, Mémoire de maîtrise. [Online]. Available at: doi:http://hdl.handle.net/11143/15848.

Picard, B. et al. (2019). Power-density to efficiency trade-off for a recuperated Inside-out Ceramic Turbine (ICT). In: *Proceedings of ASME Turbo Expo 2019*. June 2019. Phoenix AZ, USA: ASME. [Online]. Available at: doi:GT2019-91017.

PILATUS AIRCRAFT LTD. (2010). *Pilot's operating handbook PC-12/47E, MSN 545*.

Roode, M. V., Ferber, M. K. and Richerson, D. W. (2002). *Ceramic Gas Turbine Design and Test Experience*. ASME Press.

van Roode, M. (2009). Ceramic Gas Turbine Development: Need for a 10 Year Plan. *Journal of Engineering for Gas Turbines and Power*, 132 (1), p.011301. [Online]. Available at: doi:10.1115/1.3124669.

Sakakida, M. et al. (1994). *300 kW Class Ceramic Gas Turbine Development (CGT 301)*. In: 13 June 1994. The Hague Netherlands. p.V002T04A011. [Online]. Available at: doi:10.1115/94-GT-125 [Accessed 28 March 2016].

Saravanamuttoo, H. I. H. et al. (2008). *Gas Turbine Theory*. 6th ed. Pearson Education Canada.

Schober, T. and Franklin, W. (1968). *SMALL GAS TURBINE ENGINE COMPONENT TECHNOLOGY-TURBINE. VOLUME I. PHASE I SUMMARY REPORT*. CURTISS-WRIGHT CORP WOOD-RIDGE NJ.

Sellers, J. F. and Daniele, C. J. (1975). *DYNGEN: A program for calculating steady-state and transient performance of turbojet and turbofan engines*.

Takehara, I., Tatsumi, T. and Ichikawa, Y. (2002). Summary of CGT302 Ceramic Gas Turbine Research and Development Program. *Journal of Engineering for Gas Turbines and Power*, 124 (3), pp.627–635. [Online]. Available at: doi:10.1115/1.1451704.

Zok, F. W. (2016). Ceramic-matrix composites enable revolutionary gains in turbine engine efficiency. *Am Ceram Soc Bull*, 95, pp.22–28.